Journal of
MATERIALS RESEARCH

Matrix laminate composites: Realizable approximations for the effective moduli of piezoelectric dispersions

L. V. Gibiansky and S. Torquato
Department of Civil Engineering and Operations Research and Princeton Materials Institute, Princeton University, Princeton, New Jersey 08544

(Received 26 November 1997; accepted 16 March 1998)

This paper is concerned with the effective piezoelectric moduli of a special class of dispersions called matrix laminates composites that are known to possess extremal elastic and dielectric moduli. It is assumed that the matrix material is an isotropic dielectric, and the inclusions and composites are transversely isotropic piezoelectrics that share the same axis of symmetry. The exact expressions for the effective coefficients of such structures are obtained. They can be used to approximate the effective properties of any transversely isotropic dispersion. The advantages of our approximations are that they are (i) realizable, i.e., correspond to specific microstructures; (ii) analytical and easy to compute even in nondegenerate cases; (iii) valid for the entire range of phase volume fractions; and (iv) characterized by two free parameters that allow one to "tune" the approximation and describe a variety of microstructures. The new approximations are compared with known ones.

I. INTRODUCTION

Piezoelectric composite materials are important for many applications such as acoustic hydrophones, transducers, and actuators. They are especially useful because composite structures offer the opportunity for enhancement of piezoelectric performance characteristics compared to the pure piezoelectric ceramic. Often composites are the only materials capable of achieving a desired combination of properties, such as high compliance, low density, acoustic impedance matching impedance of water, and high performance characteristics.

Experiments for specific polymer/ceramic systems show[1–3] that composites with high sensitivity can be achieved by combining oriented piezoceramic rods and a soft polymer matrix. Using simple models in which the elastic and electric fields were taken to be uniform in the different phases, Haun and Newnham,[4] Chan and Unsworth,[5] and Smith[6,7] qualitatively explained the enhancement due to Poisson's ratio effect.

Rigorous prediction of the effective properties of piezoelectric-polymer composites is a technologically important but difficult problem. The effective properties are quite sensitive to the details of the microstructure due to the high contrast in the properties of the stiff piezoelectric phase with high dielectric constant, and a soft polymer with low dielectric constant.

A number of approximations have been developed to describe effective elastic and dielectric properties of composites, including the self-consistent, differential, and Mori–Tanaka schemes. Such approximations are based on the solution of the elastic and dielectric problems for a single inclusion (usually ellipsoidal) embedded in an infinite matrix subject to homogeneous fields at infinity. Recently, Dunn and Taya[8] were able to develop such approximations for piezoelectric composites. They used these approximations to study the dependence of the coupling coefficients on the phase volume fractions for composites made of piezoelectric ceramics and isotropic dielectrics for various shapes of the inclusions. Specifically, they studied composites containing spherical inclusions or cavities in a matrix, fiber-reinforced composites, and composites reinforced by elongated ellipsoids. Not surprisingly, they found that all of the approximations agree with each other at low inclusion volume fractions but diverge at higher volume fractions. They concluded that the Mori–Tanaka scheme gave the best agreement with experiments, even for moderate and high inclusion volume fractions. Kuo and Huang[9] applied the Mori–Tanaka scheme to study effective properties of the composites with spatially oriented inclusions.

Effective properties of fiber-reinforced piezocomposites were studied by Avellaneda and Swart.[10] They showed that the effective piezoelectric properties of such composites depend on only two microstructural parameters related to the transverse bulk and shear moduli, and have used a differential effective-medium approach to derive formulas for those parameters. Avellaneda and Olson[11] derived exact expressions for the effective moduli of simple (rank-one) piezoelectric laminates. Benveniste[12] studied the relation among the effective moduli of fiber-reinforced composites composed of transversely isotropic phases. Sigmund *et al.*[13] applied topology optimization techniques to design optimal piezoelectric composites.

Gibiansky and Torquato[14] studied an optimal design problem for the fiber-reinforced piezoelectric composites using the formulas developed by Avellaneda and Swart.[10] In particular, we showed that the composite with the smallest transverse bulk modulus has the best performance characteristics among all fiber-reinforced PZT-5/polymer composites. There are several types of structures that are optical in this sense. Among them are the so-called matrix laminate composites (MLC's) which realize the Hashin[15] lower bound on the effective transverse bulk modulus.

MLC's are constructed by using an iterative process. In the first stage of the process, the matrix material is layered with the inclusion phase. In the kth stage, the composite obtained from the $(k-1)$th stage is again laminated with the matrix material. The lamination directions and the phase volume fractions at each stage of the procedure are the parameters that define the effective properties of the MLC. It is assumed that the kth stage lamination is performed on a scale that is much larger than the scale of the $(k-1)$th stage, but much smaller than the size of the sample. The number of such stages in the procedure is called the rank of the MLC. We will illustrate this lamination process in the next section.

The MLC cannot be fabricated in practice, since it involves a number of sequential laminations with a wide separation of scales. However, the MLC has obvious advantages as a mathematical tool. First of all, the effective properties of an MLC can be easily computed analytically. They depend on several microstructural parameters that allow one to model composites with a high degree of anisotropy. Second, such composites often possess extremal effective properties and can serve as a benchmark in optimal design problems. Finally, the effective properties of an MLC may serve as approximations for the effective properties of dispersions, i.e., composites that consist of a matrix material reinforced with inclusions that do not cluster. Such approximations are easy to compute analytically or numerically. An additional advantage is that the structures are realizable, i.e., they correspond to specific composite microstructures.

Simple analytical expressions for the effective moduli of elastic MLC's were developed by Francfort and Murat.[16] Such composites realize the Hashin–Shtrikman[17] bounds on the effective dielectric constant of isotropic dielectrics, and the Hashin–Shtrikman[18] bounds on the effective bulk and shear moduli of isotropic elastic composites. They also realize the Hashin[15] bounds on the effective transverse bulk and shear moduli of transversely isotropic elastic composites, and the Willis[19] bounds on the effective properties of anisotropic elastic composites.[20] Anisotropic MLC's also possess extremal dielectric properties.[21–23] Effective elastic properties of transversely isotropic MLC's of two isotropic phases were studied by Lipton[24] who developed a mathematical framework to study such problems.

All of this makes MLC's perfect candidates for study with respect to their effective piezoelectric properties. In this paper we undertake such an investigation and find analytical expressions for the effective properties of transversely isotropic MLC's consisting of an isotropic dielectric (matrix) phase and a transversely isotropic piezoelectric (inclusion) phase.

The rest of the paper has the following structure: In Sec. II we describe differential equations and constitutive equations of piezoelectricity. In Sec. III we discuss general equations for the effective moduli of the MLC's and apply them to the piezoelectric problem. In Sec. IV we study the effective coupling coefficients for the piezoelectric MLC's. Specifically, we compare them with known approximations and experimental results, and study the dependence of these coefficients on the microstructural parameters, volume fraction of the piezoelectric inclusions, and stiffness of the matrix. In Sec. V we summarize the main results of our investigation.

II. STATE EQUATIONS FOR PIEZOELECTRIC MATERIALS

We start with the basic equations of piezoelectricity. For low-frequency oscillations (i.e., in the quasistatic approximation) the elasticity equations and Maxwell's equations reduce to

$$\nabla \cdot \boldsymbol{\tau} = 0, \qquad \boldsymbol{\epsilon} = \frac{1}{2}[\nabla \boldsymbol{u} + (\nabla \boldsymbol{u})^t], \tag{1}$$

and

$$\nabla \cdot \boldsymbol{D} = 0, \qquad \nabla \times \boldsymbol{E} = 0, \tag{2}$$

respectively. Here $\boldsymbol{\tau}$ and $\boldsymbol{\epsilon}$ are the stress and strain tensors, $\boldsymbol{u}$ is the displacement vector, $\boldsymbol{D}$ is the dielectric displacement, $\boldsymbol{E}$ is the electrical field, and superscript t denotes the transponded tensor, i.e.,

$$(\boldsymbol{a}^t)_{ij} = a_{ji}, \qquad (\boldsymbol{d}^t)_{kij} = d_{jik}. \tag{3}$$

These fields are coupled through constitutive relations of piezoelectricity, i.e.,

$$\begin{pmatrix} \boldsymbol{\epsilon} \\ \boldsymbol{D} \end{pmatrix} = \begin{pmatrix} \boldsymbol{S}^E & \boldsymbol{d} \\ \boldsymbol{d}^t & \boldsymbol{\sigma}^\tau \end{pmatrix} \begin{pmatrix} \boldsymbol{\tau} \\ \boldsymbol{E} \end{pmatrix}, \tag{4}$$

where $\boldsymbol{S}^E = s^E_{ijkl}$ is the fourth-order compliance tensor under short circuit boundary conditions, $\boldsymbol{d} = d_{ijk}$ is the third-order piezoelectric stress coupling tensor and $\boldsymbol{\sigma}^\tau = \sigma^\tau_{ij}$ is the second-order free-body dielectric tensor. An alternative form of the same constitutive relations is

$$\begin{pmatrix} \boldsymbol{\tau} \\ \boldsymbol{D} \end{pmatrix} = \begin{pmatrix} \boldsymbol{C}^E & e \\ \boldsymbol{e}^t & -\boldsymbol{\sigma}^\epsilon \end{pmatrix} \begin{pmatrix} \boldsymbol{\epsilon} \\ -\boldsymbol{E} \end{pmatrix}, \tag{5}$$

where $\boldsymbol{C}^E = (\boldsymbol{S}^E)^{-1}$ is the "short-circuit" stiffness tensor, $\boldsymbol{\sigma}^t = \boldsymbol{\sigma}^\tau - \boldsymbol{d}^t(\boldsymbol{S}^E)^{-1}\boldsymbol{d}$ is the clamped-body dielectric tensor, and $\boldsymbol{e} = (\boldsymbol{S}^E)^{-1}\boldsymbol{d}$ is the piezoelectric strain tensor.

The object under study is a transversely isotropic composite consisting of transversely isotropic piezoelectric phase and an isotropic dielectric phase. If the wavelength of the applied field is much larger than the spacing between piezoelectric particles, the behavior of a composite can be characterized by the averaged equations

$$\begin{pmatrix} \langle \boldsymbol{\epsilon} \rangle \\ \langle \boldsymbol{D} \rangle \end{pmatrix} = \begin{pmatrix} \boldsymbol{S}^E_* & \boldsymbol{d}_* \\ \boldsymbol{d}^t_* & \boldsymbol{\sigma}^\tau_* \end{pmatrix} \begin{pmatrix} \langle \boldsymbol{\tau} \rangle \\ \langle \boldsymbol{E} \rangle \end{pmatrix}, \tag{6}$$

where the angular brackets denote volume averaging and the index "$*$" refers to the effective properties. Similar to the relation (5), one can write the averaged constitutive relations as

$$\begin{pmatrix} \langle \boldsymbol{\tau} \rangle \\ \langle \boldsymbol{D} \rangle \end{pmatrix} = \begin{pmatrix} \boldsymbol{C}^E_* & \boldsymbol{e}_* \\ \boldsymbol{e}^t_* & -\boldsymbol{\sigma}^\epsilon_* \end{pmatrix} \begin{pmatrix} \langle \boldsymbol{\epsilon} \rangle \\ -\langle \boldsymbol{E} \rangle \end{pmatrix}, \tag{7}$$

where

$$\boldsymbol{C}^E_* = (\boldsymbol{S}^E)^{-1}_*, \qquad \boldsymbol{\sigma}^\epsilon_* = \boldsymbol{\sigma}^\tau_* - \boldsymbol{d}^t_*(\boldsymbol{S}^E_*)^{-1}\boldsymbol{d}_*, \qquad \boldsymbol{e}_* = (\boldsymbol{S}^E_*)^{-1}\boldsymbol{d}_*. \tag{8}$$

In what follows we will omit the index "$*$" in the notation for the effective properties, and use the indices p and m for the piezoelectric and matrix phase, respectively.

For a transversely isotropic material, the tensor Eq. (4) can be written in the index form

$$\begin{pmatrix} \epsilon_{11} \\ \epsilon_{22} \\ \epsilon_{33} \\ \sqrt{2}\epsilon_{23} \\ \sqrt{2}\epsilon_{13} \\ \sqrt{2}\epsilon_{12} \\ D_1 \\ D_2 \\ D_3 \end{pmatrix} = \begin{pmatrix} s_{11} & s_{12} & s_{13} & 0 & 0 & 0 & 0 & 0 & d_{13} \\ s_{12} & s_{11} & s_{13} & 0 & 0 & 0 & 0 & 0 & d_{13} \\ s_{13} & s_{13} & s_{33} & 0 & 0 & 0 & 0 & 0 & d_{33} \\ 0 & 0 & 0 & s_{55} & 0 & 0 & 0 & d_{51} & 0 \\ 0 & 0 & 0 & 0 & s_{55} & 0 & d_{51} & 0 & 0 \\ 0 & 0 & 0 & 0 & 0 & s_{66} & 0 & 0 & 0 \\ 0 & 0 & 0 & 0 & d_{51} & 0 & \sigma_{11} & 0 & 0 \\ 0 & 0 & 0 & d_{51} & 0 & 0 & 0 & \sigma_{11} & 0 \\ d_{13} & d_{13} & d_{33} & 0 & 0 & 0 & 0 & 0 & \sigma_{33} \end{pmatrix} \begin{pmatrix} \tau_{11} \\ \tau_{22} \\ \tau_{33} \\ \sqrt{2}\tau_{23} \\ \sqrt{2}\tau_{13} \\ \sqrt{2}\tau_{12} \\ E_1 \\ E_2 \\ E_3 \end{pmatrix}, \tag{9}$$

where s_{ij}, d_{ij}, and σ_{ij} are the dyadic coefficients of the tensors $\boldsymbol{S}^E$, $\boldsymbol{d}$, and $\boldsymbol{\sigma}^\tau$, respectively, in the combined elasticity-conductivity basis

$$\begin{gathered} \boldsymbol{v}_1 = \boldsymbol{ii}, \qquad \boldsymbol{v}_2 = \boldsymbol{jj}, \qquad \boldsymbol{v}_3 = \boldsymbol{kk}, \\ \boldsymbol{v}_4 = \frac{1}{\sqrt{2}}(\boldsymbol{jk} + \boldsymbol{kj}), \qquad \boldsymbol{v}_5 = \frac{1}{\sqrt{2}}(\boldsymbol{ik} + \boldsymbol{ki}), \\ \boldsymbol{v}_6 = \frac{1}{\sqrt{2}}(\boldsymbol{ij} + \boldsymbol{ji}), \\ \boldsymbol{v}_7 = \boldsymbol{i}, \qquad \boldsymbol{v}_8 = \boldsymbol{j}, \qquad \boldsymbol{v}_9 = \boldsymbol{k}, \end{gathered} \tag{10}$$

and the vector $\boldsymbol{k}$ coincides with the axis of symmetry of the transversely isotropic material. Specifically, the dyadic coefficients of the tensors $\boldsymbol{S}^E$ and $\boldsymbol{d}$ are expressed as

$$\begin{gathered} s_{ij} = \boldsymbol{v}_i : \boldsymbol{S}^E : \boldsymbol{v}_j = S_{iijj}, \\ d_{ij} = \boldsymbol{v}_i : \boldsymbol{d} \cdot \boldsymbol{v}_{j+6} = d_{iij}, \\ i, j = 1, 2, 3, \\ s_{55} = \boldsymbol{v}_5 : \boldsymbol{S}^E : \boldsymbol{v}_5 = 2S_{1313}, \\ d_{51} = \boldsymbol{v}_5 : \boldsymbol{d} \cdot \boldsymbol{v}_7 = \sqrt{2}d_{131}, \\ s_{66} = \boldsymbol{v}_6 : \boldsymbol{S}^E : \boldsymbol{v}_6 = 2S_{1212}, \end{gathered}$$

via the Cartesian coefficients S_{ijkl}, d_{ijk} of these tensors in the basis $\boldsymbol{i}, \boldsymbol{j}, \boldsymbol{k}$. The coefficients of the tensor $\boldsymbol{\sigma}$ in the basis (10) and in the Cartesian basis $\boldsymbol{i}, \boldsymbol{j}, \boldsymbol{k}$ coincide. For isotropic materials, the coefficients d_{ij} are equal to zero and

$$\begin{gathered} s_{11} = s_{22} = s_{33} = \frac{3\kappa + \mu}{9\kappa\mu}, \\ s_{12} = s_{13} = s_{23} = \frac{2\mu - 3\kappa}{18\kappa\mu}, \\ s_{44} = s_{55} = s_{66} = s_{11} - s_{12} = \frac{1}{2\mu}, \\ \sigma_{11} = \sigma_{22} = \sigma_{33} = \sigma. \end{gathered} \tag{11}$$

Here κ and μ are the bulk and shear moduli, respectively, and σ is the dielectric constant of the material.

III. MATRIX LAMINATE COMPOSITES (MLC's)

In this section we follow Lipton[24] who studied the effective properties of transversely isotropic matrix laminate composites (MLC's) of two isotropic elastic materials. The main difference between our analyses and that of Lipton[24] is that we consider transverse isotropy (rather than isotropy) of the inclusion phase, and the more complex constitutive equations for the coupled problem of piezoelectricity.

The MLC's that we consider are a special type of a high-rank laminate composite. An example of such a construction is shown in Fig. 1 where we illustrate the iterative procedure of building a rank-three MLC. One starts with a core of the inclusion phase p and layers it with a matrix material m in a layers of thickness δ^3, perpendicular to a specific direction $\boldsymbol{n}_1$ in the proportions β_1 (inclusion phase) and $1 - \beta_1$ (matrix

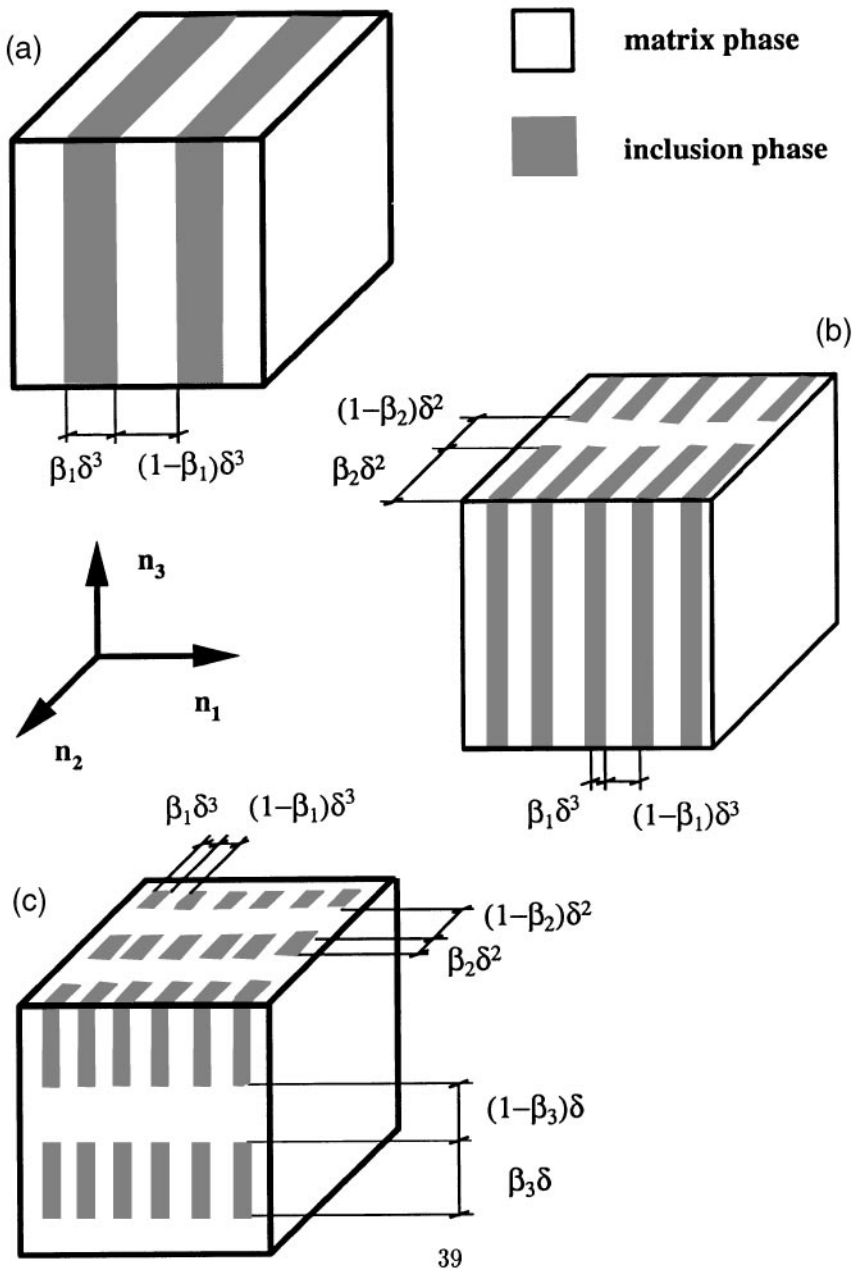

FIG. 1. Schematics of the rank-three MLC: (a) stage 1, a simple laminate composite; (b) stage 2, the fiber-reinforced rank-two MLC; (c) stage 3, the rank-three MLC. In the actual composite there is infinite separation of scales between the stages as $\delta \to 0$.

phase), respectively [see Fig. 1(a)]. Then one takes this laminate material and again layers it with the matrix material m in layers of the thickness δ^2 perpendicular to a direction $\boldsymbol{n}_2$ in the proportions β_2 (laminates obtained in the first step) and $1 - \beta_2$ (matrix phase), respectively [see Fig. 1(b)]. Then one repeats such layering one more time with the layers of the thickness δ perpendicular to the direction $\boldsymbol{n}_3$ in the proportions β_3 (the laminates obtained in the previous step) and $1 - \beta_3$ (the matrix phase), respectively [see Fig. 1(c)]. The limit of such a microgeometry when $\delta = 0$ is called a rank-three MLC. This is a simple example of a third rank lamination in which the layering directions are all orthogonal to each other. MLC's of higher rank are constructed in the same way. However, the layering directions are generally not orthogonal to each other, as described shortly below.

Simple and explicit formulas for the effective properties of the elastic MLC were developed by Francfort and Murat[16] (see also Milton[25]). Namely, consider a general constitutive equation of the form

$$\boldsymbol{j}(\boldsymbol{x}) = \boldsymbol{D}(\boldsymbol{x}) \,:\, \boldsymbol{e}(\boldsymbol{x}), \tag{12}$$

where $\boldsymbol{j}$ is the general flux, $\boldsymbol{e}$ is the field, $\boldsymbol{D}$ is the property tensor, and : denotes an appropriate contraction. Consider a rank-k MLC with the matrix phase $\boldsymbol{D}_1$ and the inclusions phase $\boldsymbol{D}_2$ taken in the proportions f_1 and f_2, respectively. The effective properties tensor $\boldsymbol{D}_*$ of such a composite is defined by the equation

$$(\boldsymbol{D}_* - \boldsymbol{D}_1)^{-1} = \frac{1}{f_2}(\boldsymbol{D}_2 - \boldsymbol{D}_1)^{-1} + \frac{f_1}{f_2}\boldsymbol{Q}\,, \qquad (13)$$

where

$$\boldsymbol{Q} = \sum_{i=1}^{k} \rho_i \boldsymbol{N}_i\,, \qquad \rho_i \geqslant 0, \qquad \sum_{i=1}^{k} \rho_i = 1\,, \qquad (14)$$

and

$$\boldsymbol{N}_i = \boldsymbol{P}_i^t : [\boldsymbol{P}_i : \boldsymbol{D}_1 : \boldsymbol{P}_i^t]^{-1} : \boldsymbol{P}_i\,. \qquad (15)$$

Here $\mathcal{P}_i = \boldsymbol{P}_i^t \boldsymbol{P}_i$ is the projection tensor on the subspace of the components of the vector $\boldsymbol{e}(\boldsymbol{x})$ that are discontinuous on the phase boundary with the normal $\boldsymbol{n}_i$. The meaning of expressions (13)–(15) will become clear when we consider the examples described shortly below. The coefficients ρ_i are defined by the structural parameters β_i at the ith step of the process via the formulas

$$\begin{aligned}
\rho_1 &= \frac{f_2}{f_1}\frac{1-\beta_1}{\beta_k\beta_{k-1}\ldots\beta_2\beta_1} = \frac{1-\beta_1}{f_1}\,,\\
\rho_2 &= \frac{f_2}{f_1}\frac{1-\beta_2}{\beta_k\beta_{k-1}\ldots\beta_2} = \frac{\beta_1(1-\beta_2)}{f_1}\\
&= \frac{\rho_1\beta_1(1-\beta_2)}{1-\beta_1}\,,\\
&\ldots\ldots\ldots\ldots\ldots\ldots\ldots\ldots\ldots\ldots\ldots\ldots\ldots\ldots\ldots\ldots\ldots\ldots\,,\\
\rho_k &= \frac{f_2}{f_1}\frac{1-\beta_k}{\beta_k} = \frac{\beta_1\beta_2\ldots\beta_{k-1}(1-\beta_k)}{f_1}\\
&= \frac{\rho_{k-1}\beta_{k-1}(1-\beta_k)}{1-\beta_{k-1}}\,,
\end{aligned} \qquad (16)$$

where we used an obvious equality (see Fig. 1)

$$\beta_k\beta_{k-1}\ldots\beta_1 = f_2\,.$$

The last term in the expression (13) is the sum of the terms $\boldsymbol{N}_i$ corresponding to the different layering directions $\boldsymbol{n}_i$; see Eq. (14). The remarkable property of the MLC and the formulas (13)–(14) is that the terms $\boldsymbol{N}_i$ that correspond to the sequential laminations with the matrix phase are additive.

Let us now apply these formulas to the effective properties of piezoelectric MLC's where the general constitutive Eq. (12) has the form (9). Consider the Cartesian basis $\boldsymbol{i}, \boldsymbol{j}, \boldsymbol{k}$, such that the vector $\boldsymbol{k}$ coincides with the axis of symmetry of the composite and the piezoelectric. Consider a lamination in the direction $\boldsymbol{n} = \boldsymbol{i}c + \boldsymbol{k}s$, where $c = \boldsymbol{n}\cdot\boldsymbol{i} = \cos\alpha$, $s = \boldsymbol{n}\cdot\boldsymbol{k} = \sin\alpha$, and α is the angle between the vectors $\boldsymbol{i}$ and the lamination direction $\boldsymbol{n}$ (see Fig. 2). Then the components

$$\begin{aligned}
\tau_{nn} = \boldsymbol{n}\cdot\boldsymbol{\tau}\cdot\boldsymbol{n}, \qquad \tau_{nb} = \boldsymbol{n}\cdot\boldsymbol{\tau}\cdot\boldsymbol{b},\\
\tau_{nt} = \boldsymbol{n}\cdot\boldsymbol{\tau}\cdot\boldsymbol{t}\,,
\end{aligned} \qquad (17)$$

of the stress field, and the components

$$E_t = \boldsymbol{E}\cdot\boldsymbol{t}\,, \qquad E_b = \boldsymbol{E}\cdot\boldsymbol{b}\,, \qquad (18)$$

of the electrical field are continuous across the phase boundary with the normal $\boldsymbol{n}$ and two orthogonal tangent vectors $\boldsymbol{t} = -\boldsymbol{i}s + \boldsymbol{k}c$ and $\boldsymbol{b} = \boldsymbol{j}$. The remaining components

$$\begin{aligned}
\tau_{tt} = \boldsymbol{t}\cdot\boldsymbol{\tau}\cdot\boldsymbol{t}\,, \qquad \tau_{bb} = \boldsymbol{b}\cdot\boldsymbol{\tau}\cdot\boldsymbol{b}\,,\\
\tau_{bt} = \boldsymbol{b}\cdot\boldsymbol{\tau}\cdot\boldsymbol{t}\,, \qquad E_n = \boldsymbol{E}\cdot\boldsymbol{n}\,,
\end{aligned} \qquad (19)$$

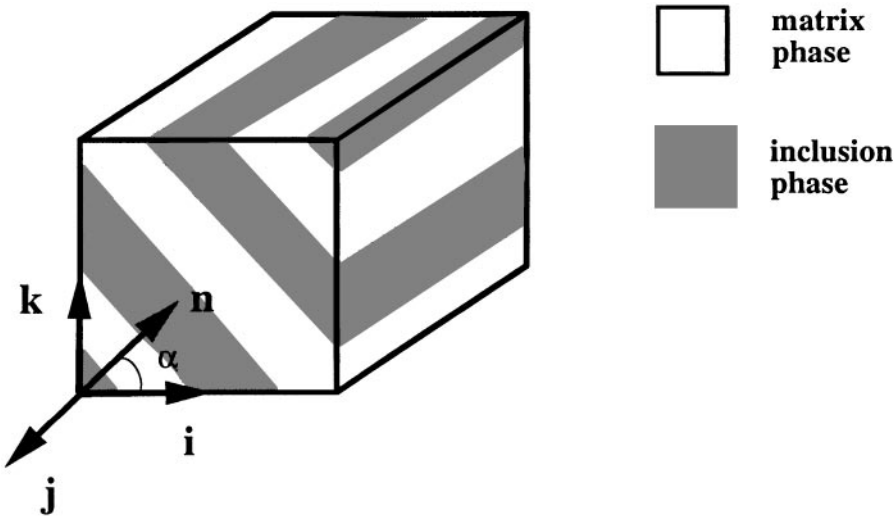

FIG. 2. Schematic picture of the stage 1 lamination.

are discontinuous, and the tensor $\boldsymbol{P} = \boldsymbol{P}(\boldsymbol{n})$ can be presented by the matrix

$$\boldsymbol{P}(\boldsymbol{n}) = \begin{pmatrix} \boldsymbol{tt} \\ \boldsymbol{bb} \\ \frac{1}{\sqrt{2}}(\boldsymbol{bt} + \boldsymbol{tb}) \\ \boldsymbol{n} \end{pmatrix} = \begin{pmatrix} s^2 & 0 & c^2 & 0 & -\sqrt{2}cs & 0 & 0 & 0 & 0 \\ 0 & 1 & 0 & 0 & 0 & 0 & 0 & 0 & 0 \\ 0 & 0 & 0 & c & 0 & -s & 0 & 0 & 0 \\ 0 & 0 & 0 & 0 & 0 & 0 & c & 0 & s \end{pmatrix} \tag{20}$$

in the basis $\boldsymbol{v}_1$–$\boldsymbol{v}_9$ associated with the vectors $\boldsymbol{i}, \boldsymbol{j}, \boldsymbol{k}$.

Now we need to evaluate the sum $\boldsymbol{Q}$ [see Eq. (13)] of the terms $\boldsymbol{N}_i$ corresponding to all lamination directions. We assume that the MLC is transversely isotropic with the vector $\boldsymbol{k}$ being the axis of the symmetry. Then any rotation around $\boldsymbol{k}$ does not change the value of the sum $\boldsymbol{Q}$ in (13). Therefore, each of the terms $\boldsymbol{N}_i$ in the expression (14) can be replaced by the group average $\hat{\boldsymbol{N}}_i$ of such terms that correspond to rotations about $\boldsymbol{k}$. Such replacement does not change the transversely isotropic tensor $\boldsymbol{Q}$. As was shown by Lipton[24]

$$\hat{\boldsymbol{N}}_i = \frac{1}{6}\sum_{l=0}^{5} \boldsymbol{R}_3^t(l\pi/6) \,:\, \boldsymbol{N}_i \,:\, \boldsymbol{R}_3(l\pi/6), \tag{21}$$

where $\boldsymbol{R}_3(\phi)$ represents the tensor of rotation by the angle ϕ about $\boldsymbol{k}$. This tensor can be written as a matrix

$$\boldsymbol{R}_3(\phi) = \begin{pmatrix} m^2 & n^2 & 0 & 0 & 0 & \sqrt{2}mn & 0 & 0 & 0 \\ n^2 & m^2 & 0 & 0 & 0 & -\sqrt{2}mn & 0 & 0 & 0 \\ 0 & 0 & 1 & 0 & 0 & 0 & 0 & 0 & 0 \\ 0 & 0 & 0 & m & -n & 0 & 0 & 0 & 0 \\ 0 & 0 & 0 & n & m & 0 & 0 & 0 & 0 \\ -\sqrt{2}mn & \sqrt{2}mn & 0 & 0 & 0 & m^2 - n^2 & 0 & 0 & 0 \\ 0 & 0 & 0 & 0 & 0 & 0 & m & n & 0 \\ 0 & 0 & 0 & 0 & 0 & 0 & -n & m & 0 \\ 0 & 0 & 0 & 0 & 0 & 0 & 0 & 0 & 1 \end{pmatrix}, \tag{22}$$

in the basis $\boldsymbol{v}_1$–$\boldsymbol{v}_9$, where

$$m = \cos\phi, \qquad n = \sin\phi. \tag{23}$$

Such a change from $\boldsymbol{N}_i$ to $\hat{\boldsymbol{N}}_i$ corresponds to the transversely isotropic MLC where any lamination direction $\boldsymbol{n}_i^{(1)}$ is accompanied by five other laminations, with the normals $\boldsymbol{n}_i^{(2)}$–$\boldsymbol{n}_i^{(6)}$ that are rotations of the vector $\boldsymbol{n}_i^{(1)}$ around the $\boldsymbol{k}$-axes by the angles $\phi_l = l\pi/6$, with equal values of the parameters $\rho_i^{(l)} = \rho_i/6$, $l = 0, \ldots, 5$.

Straightforward calculation results in the following formulas for the non-zero coefficients of the matrix $\hat{\boldsymbol{N}}_i$:

$$\begin{aligned}
\hat{N}_{11} &= \hat{N}_{22} = \frac{s_{11}^m(8 - 8c^2 + 3c^4)}{8(s_{11}^m - s_{12}^m)(s_{11}^m + s_{12}^m)}, \\
\hat{N}_{12} &= \frac{8s_{12}^m(c^2 - 1) + s_{11}^m c^4}{8(s_{11}^m - s_{12}^m)(s_{11}^m + s_{12}^m)}, \\
\hat{N}_{13} &= \hat{N}_{23} = \frac{(s_{11}^m - s_{12}^m)c^2 - s_{11}^m c^4}{2(s_{11}^m - s_{12}^m)(s_{11}^m + s_{12}^m)}, \\
\hat{N}_{33} &= \frac{s_{11}^m c^4}{(s_{11}^m - s_{12}^m)(s_{11}^m + s_{12}^m)}, \\
\hat{N}_{44} &= \hat{N}_{55} = \frac{(3s_{11}^m + s_{12}^m)c^2 - 2s_{11}^m c^4}{2(s_{11}^m - s_{12}^m)(s_{11}^m + s_{12}^m)}, \\
\hat{N}_{66} &= \frac{4(s_{11}^m + s_{12}^m)(1 - c^2) + s_{11}^m c^4}{4(s_{11}^m - s_{12}^m)(s_{11}^m + s_{12}^m)}, \\
\hat{N}_{77} &= \hat{N}_{88} = \frac{1}{2\sigma^m}c^2, \\
\hat{N}_{99} &= \frac{1}{\sigma^m}(1 - c^2),
\end{aligned} \tag{24}$$

where s_{ij}^m are the coefficients (11) of the matrix compliance tensor $\boldsymbol{S}^E$, and σ^m is the dielectric constant of the matrix phase. One can see that these expressions depend on the lamination direction only through the combinations $c^2 = \cos^2\alpha$ and $c^4 = \cos^4\alpha$. Thus, the tensor $\boldsymbol{Q}$ [see Eq. (14)] depends on the only two parameters

$$\begin{aligned}
m_2 &= \sum_{i=1}^{k} \rho_i c_i^2, \qquad m_4 = \sum_{i=1}^{k} \rho_i c_i^4, \\
c_i &\in [0,1], \qquad \sum_{i=1}^{k} \rho_i = 1,
\end{aligned} \tag{25}$$

see Eqs. (13), (14). The coefficients of the tensor $\boldsymbol{Q}$ are given by Eqs. (24) where one should replace $\hat{N}_{ij}$ by $\boldsymbol{Q}_{ij}$, replace c^2 by m_2, and replace c^4 by m_4. Lipton[24] showed that the parameters m_2 and m_4 obey the restrictions

$$0 \leqslant m_4 \leqslant m_2 \leqslant \sqrt{m_4} \leqslant 1 \tag{26}$$

for any choice of the lamination directions ($c_i \in [0,1]$) and structural parameters ρ_i. He also proved that one can attain any admissible pair (m_2, m_4) [i.e., any pair (m_2, m_4) subject to the restrictions (26)] by combining at most seven lamination directions.

Figure 3 schematically illustrates the structures that correspond to some special cases of the parameters m_2 and m_4. It is easy to see that the values

$$m_2 = m_4 = 0 \tag{27}$$

correspond to the simple rank-one lamination in the $\boldsymbol{k}$ direction. On the other hand, the values

$$m_2 = m_4 = 1 \tag{28}$$

correspond to microgeometries that have cylindrical symmetry. *Any such composite is equivalent with respect to the effective properties to the transversely*

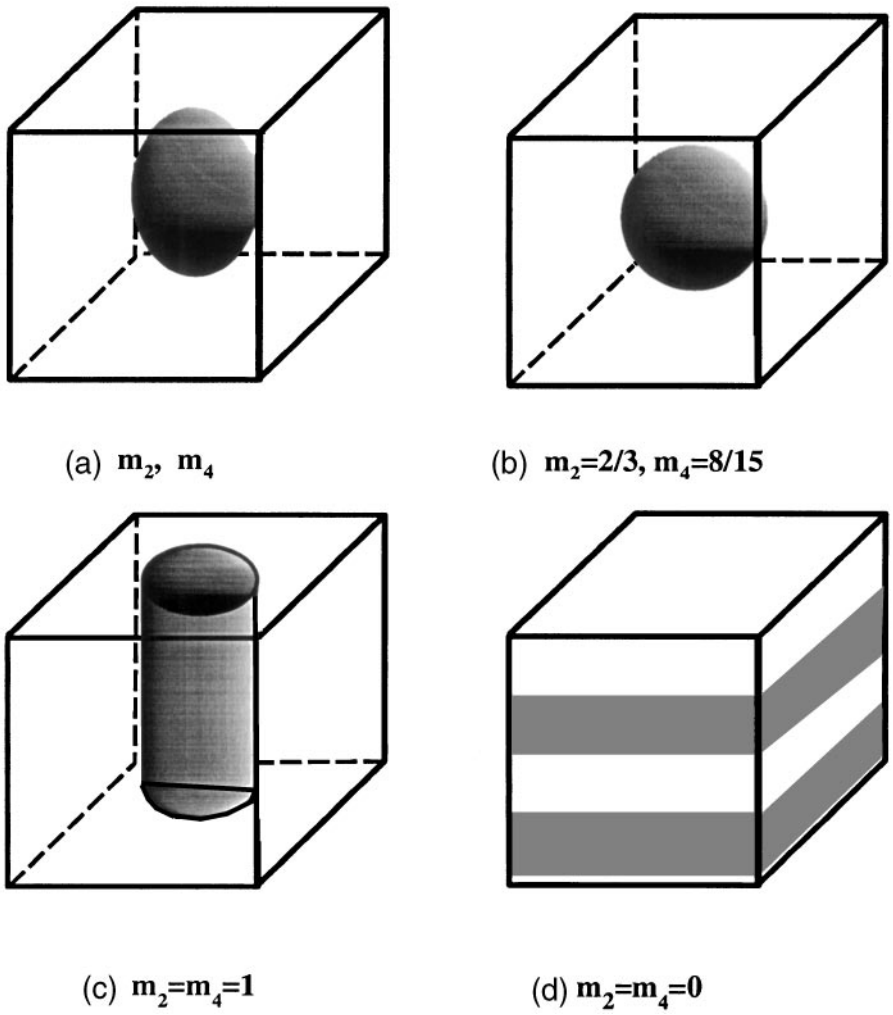

FIG. 3. Schematic picture of the MLC's: (a) a general transversely isotropic case, (b) spherically symmetric case, (c) cylindrical case, and (d) simple laminate composite.

isotropic rank-three MLC.[24] Such laminates most closely correspond to distributions of aligned circular cylinders that are statistically transversely isotropic.

One can also check that the values

$$m_2 = 2/3\,, \qquad m_4 = 8/15 \tag{29}$$

correspond to the isotropic tensor $\hat{\boldsymbol{Q}} = \sum_{i=1}^{k} \hat{N}_i$, i.e., to spherically symmetric rank-seven lamination. We will use the spherically symmetric lamination with the parameters (29) to model microstructures that are statistically isotropic. They are not isotropic with respect to the piezoelectric properties since all of the piezoelectric inclusions are poled in one specific direction. However, the microgeometry of the composite is statistically isotropic. This example most closely corresponds to a statistically isotropic distribution of spherical particles.

Remark: The effective piezoelectric properties of cylindrical fiber-reinforced composites were studied by Avellaneda and Swart[10] by using the differential effective medium approximation. They found that the effective properties of such cylindrical transversely isotropic composites depend only on two parameters (related to the effective transverse bulk and shear moduli). In our earlier paper,[14] we used the structures that realize the Hashin–Shtrikman transverse bulk modulus bounds. The cylindrical ($m_2 = m_4 = 1$) MLC considered in this paper is an example of such a structure.

Let us now reduce the dimensions of the matrices involved in the formulas by decomposing the equality (13) (involving for the piezoelectric case 9 by 9 transversely isotropic matrices of the form (9) which share the same axis of symmetry) into the set of smaller matrix equalities. Every transversely isotropic matrix $\boldsymbol{D}$ of the form (9) can be transformed as

$$\overline{\boldsymbol{D}} = \boldsymbol{G} \,:\, \boldsymbol{D} \,:\, \boldsymbol{G}^t, \tag{30}$$

where

$$\boldsymbol{G} = \begin{pmatrix} 1/\sqrt{2} & -1/\sqrt{2} & 0 & 0 & 0 & 0 & 0 & 0 & 0 \\ 1/\sqrt{2} & 1/\sqrt{2} & 0 & 0 & 0 & 0 & 0 & 0 & 0 \\ 0 & 0 & 1 & 0 & 0 & 0 & 0 & 0 & 0 \\ 0 & 0 & 0 & 0 & 0 & 0 & 0 & 0 & 1 \\ 0 & 0 & 0 & 1 & 0 & 0 & 0 & 0 & 0 \\ 0 & 0 & 0 & 0 & 0 & 0 & 0 & 1 & 0 \\ 0 & 0 & 0 & 0 & 1 & 0 & 0 & 0 & 0 \\ 0 & 0 & 0 & 0 & 0 & 0 & 1 & 0 & 0 \\ 0 & 0 & 0 & 0 & 0 & 1 & 0 & 0 & 0 \end{pmatrix}. \tag{31}$$

Then the matrix $\overline{\boldsymbol{D}}$ is a block-diagonal matrix of the form

$$\overline{\boldsymbol{D}} = \begin{pmatrix} s_{11} - s_{12} & 0 & 0 & 0 & 0 & 0 & 0 & 0 & 0 \\ 0 & s_{11} + s_{12} & \sqrt{2}s_{13} & \sqrt{2}d_{13} & 0 & 0 & 0 & 0 & 0 \\ 0 & \sqrt{2}s_{13} & s_{33} & d_{33} & 0 & 0 & 0 & 0 & 0 \\ 0 & \sqrt{2}d_{13} & d_{33} & \sigma_{33} & 0 & 0 & 0 & 0 & 0 \\ 0 & 0 & 0 & 0 & s_{55} & d_{51} & 0 & 0 & 0 \\ 0 & 0 & 0 & 0 & d_{51} & \sigma_{11} & 0 & 0 & 0 \\ 0 & 0 & 0 & 0 & 0 & 0 & s_{55} & d_{51} & 0 \\ 0 & 0 & 0 & 0 & 0 & 0 & d_{51} & \sigma_{11} & 0 \\ 0 & 0 & 0 & 0 & 0 & 0 & 0 & 0 & s_{66} \end{pmatrix}. \tag{32}$$

Similarly, one can transform any of the matrices that enter the formula (13). Thus it can be reduced to a set of the equalities

$$\frac{1}{\eta^* - \eta^m} = \frac{1}{f_2}\frac{1}{\eta^p - \eta^m} + \frac{f_1}{f_2}q_{11}, \tag{33}$$

(where $\eta^* = s_{11}^* - s_{12}^*$, $\eta^i = s_{11}^i - s_{12}^i$, $i = m, p$)

$$\frac{1}{s_{66}^* - s_{66}^m} = \frac{1}{f_2}\frac{1}{s_{66}^p - s_{66}^m} + \frac{f_1}{f_2}q_{99}, \tag{34}$$

$$\begin{pmatrix} s_{55}^* - s_{55}^m & d_{51}^* \\ d_{51}^* & \sigma_{11}^* - \sigma_{11}^m \end{pmatrix}^{-1} = \frac{1}{f_2}\begin{pmatrix} s_{55}^p - s_{55}^m & d_{51}^p \\ d_{51}^p & \sigma_{11}^p - \sigma_{11}^m \end{pmatrix}^{-1} + \frac{f_1}{f_2}\begin{pmatrix} q_{55} & 0 \\ 0 & q_{66} \end{pmatrix}, \tag{35}$$

and

$$\begin{pmatrix} \gamma^* - \gamma^m & \sqrt{2}\left(s_{13}^* - s_{13}^m\right) & \sqrt{2}d_{13}^* \\ \sqrt{2}\left(s_{13}^* - s_{13}^m\right) & s_{33}^* - s_{33}^m & d_{33}^* \\ \sqrt{2}d_{13}^* & d_{33}^* & \sigma_{33}^* - \sigma_{33}^m \end{pmatrix}^{-1} = \frac{1}{f_2}\begin{pmatrix} \gamma^p - \gamma^m & \sqrt{2}(s_{13}^p - s_{13}^m) & \sqrt{2}d_{13}^p \\ \sqrt{2}(s_{13}^p - s_{13}^m) & s_{33}^p - s_{33}^m & d_{33}^p \\ \sqrt{2}d_{13}^p & d_{33}^p & \sigma_{33}^p - \sigma_{33}^m \end{pmatrix}^{-1} + \frac{f_1}{f_2}\begin{pmatrix} q_{22} & q_{23} & 0 \\ q_{23} & q_{33} & 0 \\ 0 & 0 & q_{44} \end{pmatrix}, \tag{36}$$

(where $\gamma^* = s_{11}^* + s_{12}^*$, $\gamma^i = s_{11}^i + s_{12}^i$, $i = m, p$). Here indices m and p refer to the properties of the matrix and piezoelectric inclusions, respectively, and the parameters q_{ij} are given by

$$\begin{aligned} q_{11} &= \sum_{i=1}^{k}\rho_i[\hat{N}_{11}(c_i) - \hat{N}_{12}(c_i)] \\ &= \frac{4(s_{11}^m + s_{12}^m)(1 - m_2) + s_{11}^m m_4}{4(s_{11}^m - s_{12}^m)(s_{11}^m + s_{12}^m)}, \\ q_{22} &= \sum_{i=1}^{k}\rho_i[\hat{N}_{11}(c_i) - \hat{N}_{12}(c_i)] \\ &= \frac{2(s_{11}^m - s_{12}^m)(1 - m_2) + s_{11}^m m_4}{2(s_{11}^m - s_{12}^m)(s_{11}^m + s_{12}^m)}, \\ q_{23} &= \sum_{i=1}^{k}\sqrt{2}\rho_i\hat{N}_{13}(c_i) \\ &= \frac{(s_{11}^m - s_{12}^m)m_2 - s_{11}^m m_4}{2(s_{11}^m - s_{12}^m)(s_{11}^m + s_{12}^m)}, \\ q_{33} &= \sum_{i=1}^{k}\rho_i\hat{N}_{33}(c_i) = \frac{s_{11}^m m_4}{(s_{11}^m - s_{12}^m)(s_{11}^m + s_{12}^m)}, \\ q_{44} &= \sum_{i=1}^{k}\rho_i\hat{N}_{99}(c_i) = \frac{1}{\sigma}(1 - m_2), \\ q_{55} &= \sum_{i=1}^{k}\rho_i\hat{N}_{44}(c_i) = \frac{(3s_{11}^m + s_{12}^m)m_2 - 2s_{11}^m m_4}{2(s_{11}^m - s_{12}^m)(s_{11}^m + s_{12}^m)}, \\ q_{66} &= \sum_{i=1}^{k}\rho_i\hat{N}_{77}(c_i) = \frac{m_2}{2\sigma}, \\ q_{99} &= \sum_{i=1}^{k}\rho_i\hat{N}_{66}(c_i) = \frac{4(s_{11}^m + s_{12}^m)(1 - m_2) + s_{11}^m m_4}{4(s_{11}^m - s_{12}^m)(s_{11}^m + s_{12}^m)}. \end{aligned} \tag{37}$$

Equations (33)–(37) define the effective properties of the transversely isotropic matrix piezoelectric composite. In addition to the phase properties and volume fractions, they depend on two microstructural parameters m_2 and m_4 subject to the restrictions (26).

The advantages of such a representation over the more traditional effective-medium, differential effective-medium, and Mori–Tanaka approximation schemes are that it is (i) realizable, i.e., the formulas exactly correspond to some microstructures; (ii) analytical and easy to compute; (iii) valid for the entire range of volume fractions; (iv) possesses two free parameters m_2 and m_4 that can be tuned so as to yield the approximation formulas to achieve better agreement with experimental results.

The last statement should be not understood as an attempt to fit the theory to any experimental data. We mean that the experimental measurements of the composite properties at some inclusion volume fraction can be used to "tune" the approximation to fit the data

at the given volume fraction. Then our approximation would allow one to predict the piezoelectric properties of the composite *at any phase volume fractions.* Moreover, the same values of the parameters can be used to approximate the properties of composite with another pair of phase properties, but with similar geometrical structure (i.e., similar inclusions shapes and similar inclusions size distribution). Such tuning might be necessary since the approximation corresponds to some specific ideal structure (MLC) that differs from the microstructure of any real experimental system. The idea is that for a wide class of the microstructures there may be an equivalent MLC that corresponds closely to the experimental dispersion of piezoelectric particles in an isotropic polymer.

Sometimes it is convenient to present constitutive equations of the piezoelectricity in the form (5). All of the calculations can be repeated yielding the formulas

$$\frac{1}{2\mu^* - 2\mu^m} = \frac{1}{f_2}\frac{1}{2\mu^p - 2\mu^m} + \frac{f_1}{f_2}h_{11}, \qquad (38)$$

$$\frac{1}{c^*_{66} - c^m_{66}} = \frac{1}{f_2}\frac{1}{c^p_{66} - c^m_{66}} + \frac{f_1}{f_2}h_{99}, \qquad (39)$$

$$\begin{pmatrix} c^*_{55} - c^m_{55} & e^*_{51} \\ e^*_{51} & -(\sigma^*_{11} - \sigma^m_{11}) \end{pmatrix}^{-1} = \frac{1}{f_2}\begin{pmatrix} c^p_{55} - c^m_{55} & e^p_{51} \\ e^p_{51} & -(\sigma^p_{11} - \sigma^m_{11}) \end{pmatrix}^{-1} + \frac{f_1}{f_2}\begin{pmatrix} h_{55} & 0 \\ 0 & h_{66} \end{pmatrix}, \qquad (40)$$

$$\begin{pmatrix} 2(K^* - K^m) & \sqrt{2}(c^*_{13} - c^m_{13}) & \sqrt{2}e^*_{13} \\ \sqrt{2}(c^*_{13} - c^m_{13}) & c^*_{33} - c^m_{33} & e^*_{33} \\ \sqrt{2}e^*_{13} & e^*_{33} & -(\sigma^*_{33} - \sigma^m_{33}) \end{pmatrix}^{-1} = \frac{1}{f_2}\begin{pmatrix} 2(K^p - K^m) & \sqrt{2}(c^p_{13} - c^m_{13}) & \sqrt{2}e^p_{13} \\ \sqrt{2}(c^p_{13} - c^m_{13}) & c^p_{33} - c^m_{33} & e^p_{33} \\ \sqrt{2}e^p_{13} & e^p_{33} & -(\sigma^p_{33} - \sigma^m_{33}) \end{pmatrix}^{-1} + \frac{f_1}{f_2}\begin{pmatrix} h_{22} & h_{23} & 0 \\ h_{23} & h_{33} & 0 \\ 0 & 0 & h_{44} \end{pmatrix}, \qquad (41)$$

where

$$2\mu^* = c^*_{11} - c^*_{12}, \quad 2\mu^i = c^i_{11} - c^i_{12}, \quad i = m, p;$$
$$2K^* = c^*_{11} + c^*_{12}, \quad 2K^i = c^i_{11} + c^i_{12}, \quad i = p, m, \qquad (42)$$

and

$$h_{11} = \frac{4c^m_{11}m_2 - (c^m_{11} + c^m_{12})m_4}{4c^m_{11}(c^m_{11} - c^m_{12})},$$
$$h_{22} = \frac{2c^m_{11}m_2 - (c^m_{11} + c^m_{12})m_4}{2c^m_{11}(c^m_{11} - c^m_{12})},$$
$$h_{23} = \frac{\sqrt{2}(c^m_{11} + c^m_{12})(m_4 - m_2)}{2c^m_{11}(c^m_{11} - c^m_{12})},$$
$$h_{33} = \frac{c^m_{11} - c^m_{12} + 2c^m_{12}m_2 - (c^m_{11} + c^m_{12})m_4}{c^m_{11}(c^m_{11} - c^m_{12})},$$
$$h_{44} = -\frac{1}{\sigma^m}(1 - m_2),$$
$$h_{55} = \frac{2c^m_{11} - (3c^m_{11} + 2c^m_{12})m_2 + 2(c^m_{11} + c^m_{12})m_4}{2c^m_{11}(c^m_{11} - c^m_{12})},$$
$$h_{66} = -\frac{m_2}{2\sigma^m},$$
$$h_{99} = \frac{4c^m_{11}m_2 - (c^m_{11} + c^m_{12})m_4}{4c^m_{11}(c^m_{11} - c^m_{12})}. \qquad (43)$$

Note that for an isotropic phase,

$$c_{11} = c_{22} = c_{33} = \frac{3\kappa + 4\mu}{3},$$
$$c_{12} = c_{13} = c_{23} = \frac{3\kappa - 2\mu}{3},$$
$$c_{44} = c_{55} = c_{66} = c_{11} - c_{12} = 2\mu,$$

where κ and μ are the bulk and shear moduli, respectively.

If both matrix and inclusion phases are isotropic, then the resulting expressions agree with those obtained by Lipton[24] for the transversely isotropic composite of two isotropic elastic phases.

Our goal is to study dependences of the piezoelectric moduli of the MLC on the microstructural parameters m_2 and m_4, on the volume fraction of the piezoelectric f_2, and on the stiffness of the matrix phase.

IV. EFFECTIVE PROPERTIES OF PIEZOELECTRIC MLC's

Now we have in hand the analytical expressions for the effective properties of transversely isotropic MLC's consisting of a polymer matrix and piezoelectric inclusions. In this section we compare this approximation with other approximations for the effective properties of the piezoelectric composites and study the dependence of the properties on the microstructural parameters m_2 and m_4.

A. Comparison with known approximations

Dunn and Taya[8] used the solution of the boundary-value problem for a piezoelectric ellipsoid embedded in a piezoelectric matrix to study the self-consistent, Mori–Tanaka, and differential approximations for two-phase piezoelectric composites. We will compare our formulas with their results. Table I contains the phase moduli for the composites studied by Dunn and Taya[8]; we will use the same values in our comparison.

We begin by comparing results for an epoxy composite reinforced by spherical PZT-5 particles. Figure 4

TABLE I. Electrostatic material properties.

Material	c_{11} GPa	c_{12} GPa	c_{13} GPa	c_{33} GPa	c_{55} GPa	e_{31} C/m^2	e_{33} C/m^2	e_{15} C/m^2	σ_{11} σ_0	σ_{33} σ_0
PZT-7A$_1$	148	76.2	74.2	131	25.4	−2.1	9.5	9.2	460	235
PZT-7A$_2$	148	76.2	74.2	131	25.4	−2.1	12.1	9.2	460	235
PZT-5	121	75.4	75.2	111	21.1	−5.4	15.8	12.3	916	830
Epoxy	8.0	4.4	4.4	8.0	1.8	0	0	0	4.2	4.2
Polymer	3.86	2.57	2.57	3.86	0.64	0	0	0	9.0	9.0

$\sigma_0 = 8.8510^{-12}$ (C^2/Nm^2) is a permittivity of free space.

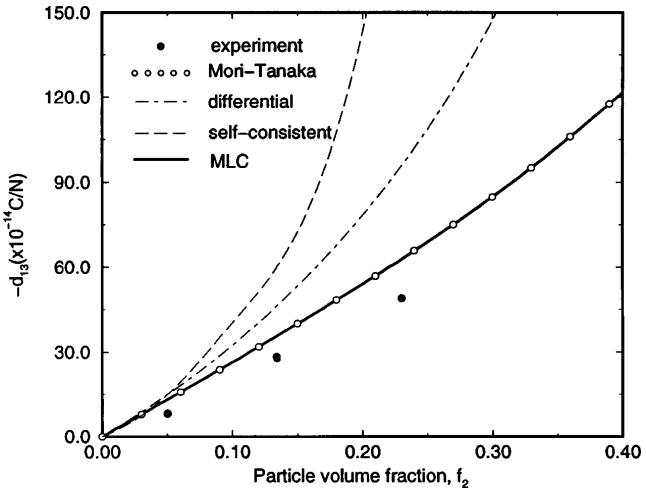

FIG. 4. The effective piezoelectric coefficient d_{13} of a PZT-5 spherical-particle-reinforced epoxy composite as a function of the particle volume fraction f_2. Comparison of our realizable approximation with the approximations computed by Dunn and Taya[8] and the experimental results of Furukawa *et al.*[26]

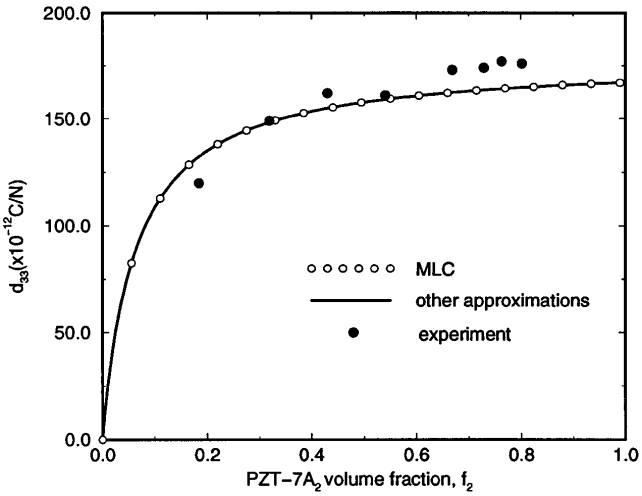

FIG. 5. The effective piezoelectric coefficient d_{33} of a PZT-7A$_2$ fiber-reinforced epoxy composite as a function of the fiber volume fraction f_2. Comparison of our realizable approximation with the approximations computed by Dunn and Taya[8] and experimental results of Chan and Unsworth.[5]

depicts the volume-fraction dependence of the d_{13} coefficient for such a composite. The thin curves correspond to the different approximations computed by Dunn and Taya.[8] We model such a composite by the MLC with the parameter values

$$m_2 = 2/3, \qquad m_4 = 8/15\,, \tag{44}$$

which correspond to the isotropic tensor $\hat{\boldsymbol{Q}}$ in (14). The bold curve represents our data for MLC's, and the black circles are the experimental results of Furukawa *et al.*[26] as given by Dunn and Taya.[8] One can see that our approximations is in agreement with the experimental results and previously known approximations.

Figure 5 shows similar comparisons for composites of PZT-7A$_2$ fiber-reinforced epoxy composite. Fiber-reinforced composites correspond to MLC's with microstructural parameters

$$m_2 = \cos^2(0) = 1, \qquad m_4 = \cos^4(0) = 1\,. \tag{45}$$

The black circles are the experimental results of Chan and Unsworth.[5] The bold curve represents the dependence of the d_{33} coefficient on the volume fraction as given by our formulas for the MLC's. The unfilled circles correspond to the Dunn and Taya[8] approximations (differential, Mori–Tanaka, self-consistent) that coincide in this case. Note that in order to get agreement with the experimental results, Dunn and Taya corrected the phase moduli of the PZT-7A$_1$ ceramic, given by Furukawa *et al.*[26] taking into account the value of the d_{33} coefficient measured by Chan and Unsworth. This corresponds to the moduli of PZT-7A$_2$ given in Table I. One can see that for fiber-reinforced composites, our formulas are in good agreement with the experimental results and known approximations.

Figures 6(a) and 6(b) give the dependence of the effective piezoelectric moduli e_{13} and e_{33}, respectively, of PZT-7A$_1$ short-fiber-reinforced epoxy composites as a function of the fiber volume fraction. Dunn and Taya[8] modeled such a microgeometry by considering (in their approximation schemes) prolate spheroids with aspect ratio equal to 10. Their results are shown by the thin curves (the differential and self-consistent approximations) or by the unfilled circles (the Mori–Tanaka approximation).

We can model the same structure by the MLC using several different combinations of the parameters

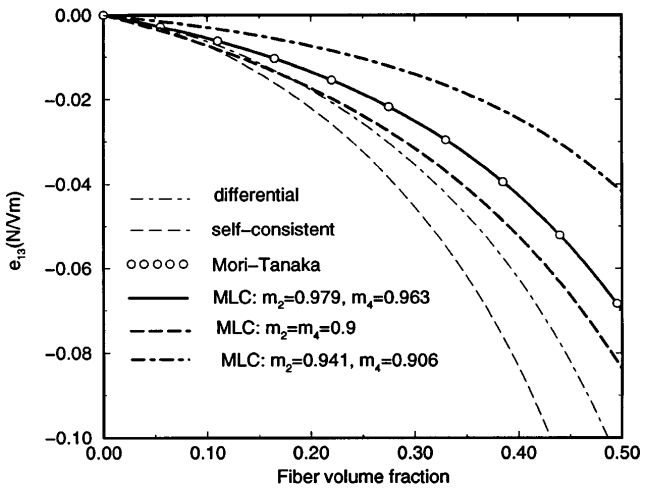

(a)

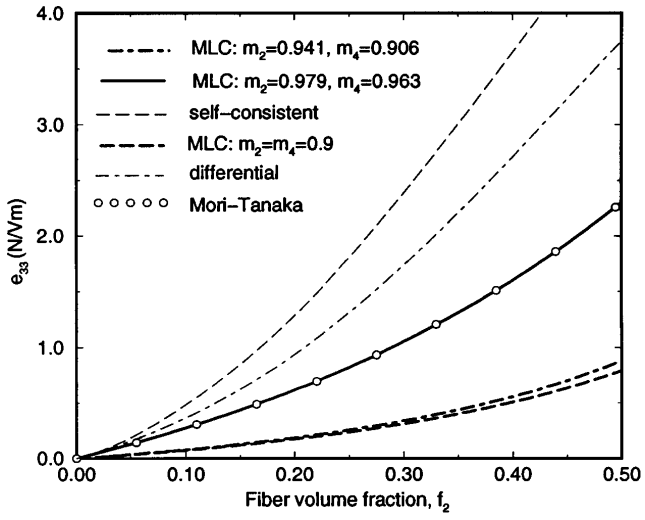

(b)

FIG. 6. The effective piezoelectric coefficient e_{13} (a) and e_{33} (b) of a PZT-7A$_1$ short-fiber reinforced epoxy composite with the aspect ratio $a = 10$ as a function of the fiber volume fraction f_2. Comparison of our realizable approximations with the approximations computed by Dunn and Taya.[8]

m_2 and m_4. One way is to assign the weight $\rho_2 = 9/10$ to the laminations in the direction $\alpha = 0$ and weight $\rho_1 = 1/10$ to the laminations in the direction $\alpha_2 = \pi/2$; in this case

$$m_2 = \frac{9}{10}\cos^2(0) + \frac{1}{10}\cos^2(\pi/2) = \frac{9}{10}\,,$$
$$m_4 = \frac{9}{10}\cos^4(0) + \frac{1}{10}\cos^4(\pi/2) = \frac{9}{10}\,. \quad (46)$$

The results are depicted as bond dashed curves in Figs. 6(a) and 6(b). One can see that such an approximation for the e_{13}-coefficient lies between the Mori–Tanaka and differential approximations. However, the approximation for the e_{33}-coefficient is very sensitive to the details of the microstructure, i.e., to the microstructural parameters m_2 and m_4.

An alternative way to model such composites is to assume that the parameters $\rho(\phi)$ in the formulas (13)–(16) are distributed according to the eccentricity of the ellipsoidal inclusions

$$\rho_*(\phi) = \frac{A}{\sqrt{(c/a)^2 + (s/b)^2}}\,, \qquad c = \cos\phi\,,$$
$$s = \sin\phi\,, \qquad a = 0.9\,, \qquad b = 0.1\,. \quad (47)$$

Here A is some constant chosen to ensure that the integral of $\rho(\phi)$ over $\phi \in [0, \pi/2]$ is equal to 1. Such an approximation results in the formulas

$$m_2 = \int_0^{\pi/2} \rho_*^2(\phi)\cos^3(\phi)\,d\phi \;\Big/\; \int_0^{\pi/2} \rho_*^2(\phi)\cos(\phi)\,d\phi = 0.941\,,$$
$$m_4 = \int_0^{\pi/2} \rho_*^2(\phi)\cos^5(\phi)\,d\phi \;\Big/\; \int_0^{\pi/2} \rho_*^2(\phi)\cos(\phi)\,d\phi = 9.06\,, \quad (48)$$

which corresponds to the bold dotted curves in Figs. 6(a) and 6(b). One can see that these curves lie rather far from the traditional approximations in this case.

We are not aware of experimental results that would allow us to choose among different approximations for the effective moduli of the short-fiber-reinforced composite. Note that if $\rho_* = 1$ (symmetric lamination), then the expressions (48) return $m_2 = 2/3$, $m_4 = 8/15$, in agreement with (44).

Let us now demonstrate how to tune our approximation to fit the experimental data. Assume, for example, that in the composite the values of the parameters e_{13} and e_{33} correspond to the Mori–Tanaka approximation given by Dunn and Taya [Figs. 6(a) and 6(b)]. Assume also that one can measure the values of these parameters at the inclusion volume fraction $f_2 = 0.5$, and the measurements results in the values $e_{13} = -0.07$ and $e_{33} = 2.3$, as one can see on Figs. 6(a) and 6(b). Let us choose the parameters

$$m_2 = 0.979, \qquad m_4 = 0.963\,, \quad (49)$$

so that the resulting values of the piezoelectric coefficients of the MLC ($e_{13} = -0.07$ and $e_{33} = 2.3$) coincide with the "experiment" at the point $f_2 = 0.5$. The corresponding approximation [bold solid curves in Figs. 6(a) and 6(b)] is realizable since the parameters (49) satisfy the restrictions (26), and perfectly agree with the "experimental" curve.

We emphasize that the parameters m_2 and m_4 are purely geometrical. Let us assume that for some piezoelectric composite with the specific phase properties, volume fractions, characteristic shape, and size distribution of the inclusions, one can identify the values of the parameters that agree with the experimental data.

Then the same values of the parameters can be used to approximate the effective properties of the composites made of arbitrary phases, taken in arbitrary volume fractions, provided the shapes of the inclusions are of the same type and size distribution as in the "reference" composite.

B. Mori–Tanaka scheme and the MLC's

We have seen in the previous section that there is good agreement between our formulas and the Mori–Tanaka approximation for the effective properties of the fiber-reinforced and spherical-particle-reinforced piezoelectric composites. In this section we discuss the intrinsic reasons for such agreement.

As was found by Weng,[27] the Mori–Tanaka approximation for the effective properties of an *elastic* composite consisting of a matrix material and aligned ellipsoidal inclusions, coincide with the lower Hashin–Shtrikman bound if the matrix material is weaker than the inclusion phase, and coincide with the upper Hashin–Shtrikman bound if the matrix material is stronger than the inclusion phase. The Hashin–Shtrikman bounds for anisotropic composites were found by Willis.[19]

On the other hand, Avellaneda[20] has shown that there exist MLC's that realize the same bounds. It is now immediately clear that the Mori–Tanaka approximation *for elastic composites consisting of a matrix and aligned ellipsoidal inclusions* correspond to some MLC's. The same agreement between the Mori–Tanaka approximation and the effective properties of the MLC's can be found for conducting composites of aligned ellipsoidal inclusions in a matrix.

One can conjecture that the Mori–Tanaka approximation for the effective properties of any composite consisting of aligned ellipsoidal inclusions in a matrix, corresponds to some MLC. One can easily prove the aforementioned statement in the particular case of a piezoelectric composite consisting of piezoelectric inclusions in an *isotropic* matrix. Indeed, the formulas for the Mori–Tanaka approximation can be presented in the form (13) with

$$\boldsymbol{Q} = \boldsymbol{S} : \boldsymbol{D}_1^{-1}, \tag{50}$$

where $\boldsymbol{S}$ is the Eshelby tensor.[8] If matrix phase is isotropic, then the tensor (50) does not contain coupling terms. In fact, it is a direct sum of the part corresponding to the elasticity problem and the part corresponding to the electric problem. We just mentioned that for both of these problems one can find MLC's with the tensors $\boldsymbol{Q}$ equal to the corresponding tensor $\boldsymbol{S} : \boldsymbol{D}_1^{-1}$ in the Mori–Tanaka approximation. Therefore, for the piezoelectric problem with an isotropic matrix, these tensors also coincide, leading to the conclusion that the Mori–Tanaka approximation coincides with the effective properties of some MLC's in this case.

We explicitly checked for such a coincidence for the composite reinforced by the spheroidal particles, where the formulas for the Mori–Tanaka approximation are available in the literature.[28,29] We found out that our approximation coincides with the Mori–Tanaka scheme if the parameters m_2, m_4 are related to the geometrical parameters of the spheroidal inclusions as follows:

$$m_2 = g, \qquad m_4 = \frac{g + 2a^2 - 4ga^2}{2(1 - a^2)}, \tag{51}$$

where $a = l/d$ is the aspect ratio of the spheroidal inclusions (l and d are the vertical and axial dimensions, respectively) and

$$g = \frac{a}{(a^2 - 1)^{3/2}} \left(a(a^2 - 1)^{1/2} - \cosh^{-1}(a)\right), \quad \text{if } a \geqslant 1 \text{ (prolate shape)},$$
$$g = \frac{a}{(1 - a^2)^{3/2}} \left(\cos^{-1}(a) - a(1 - a^2)^{1/2}\right), \quad \text{if } a \leqslant 1 \text{ (oblate shape)}. \tag{52}$$

For the model of a short-fiber-reinforced composite in which the aspect ratio $a = 10$, these expressions return

$$m_2 = 0.9797, \qquad m_4 = 0.9642, \tag{53}$$

which are in perfect agreement with our numerical calculations (49). Similarly, $a = \infty$ (fiber-reinforced composite) corresponds to the values $m_2 = m_4 = 1$, and the limit of the expressions (51) when $a = 1$ (spherical particles) results in $m_2 = 2/3$, $m_4 = 8/15$, which are in agreement with (45) and (44), respectively.

Thus, we have proved that the Mori–Tanaka approximation for the effective moduli of the composite with aligned spheroidal inclusions can be realized by MLC's. Moreover, we have provided a simple parameterization of the admissible effective properties via the parameters m_2 and m_4. In contrast, the corresponding spheroidal inclusion has only one free parameter (aspect ratio a). Therefore, the Mori–Tanaka scheme describes a smaller set of effective properties than do the MLC's.

C. Effect of microstructure and matrix stiffness on effective properties

In this section, we investigate the dependence of the piezoelectric properties, such as the coupling coefficients d_{13} and d_{33}, on the microstructural parameters m_2, m_4, and the piezoelectric inclusions volume fraction f_2. As an example, we consider an epoxy matrix with PZT-5 ceramic inclusions.

First, let us fix the volume fraction $f_2 = 0.1$ and study the dependence of the properties on the microstructural parameters m_2 and m_4 subject to the restriction (26). Figure 7(a) shows the dependence of d_{13} and

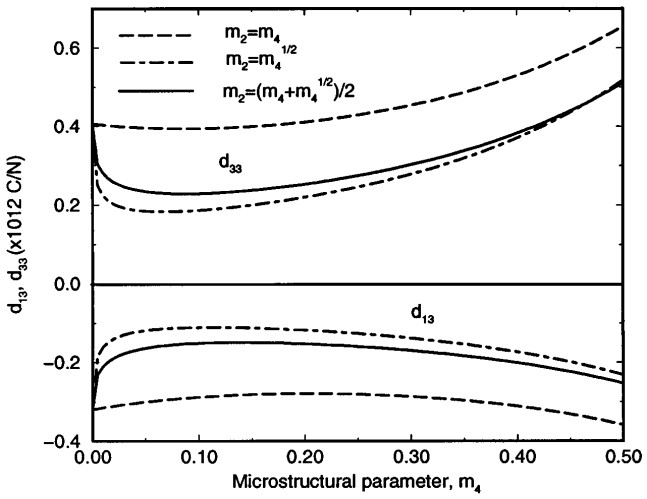

(a)

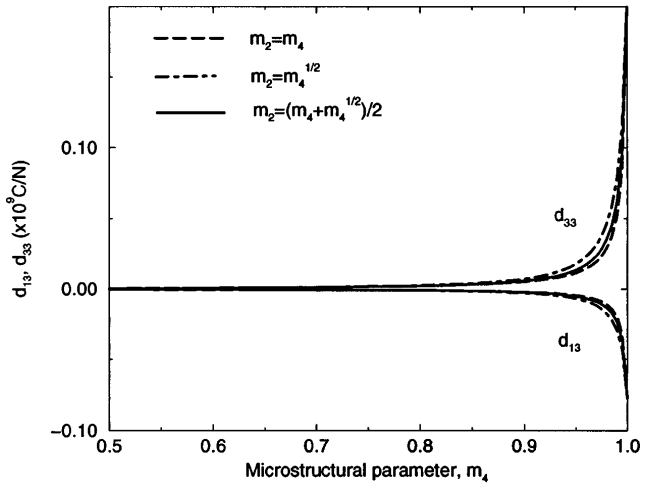

(b)

FIG. 7. The effective piezoelectric coefficients d_{13} and d_{33} of a PZT-5A/epoxy composite as a function of the microstructural parameter m_4 for fixed value $f_2 = 0.1$ of the piezoelectric volume fraction f_2: (a) for small values of the parameter $m_4 \in [0, 0.5]$; (b) for larger values of the parameter $m_4 \in [0.5, 1]$. The parameter m_2 is taken to be a function (specific for each of the curves) of the parameter m_4.

d_{33}, respectively, on the parameter $m_4 \in [0, 0.5]$ when $m_2 = m_4$ (the solid curves), $m_2 = \sqrt{m_4}$ (the bold dashed curves), and $m_2 = (m_4 + \sqrt{m_4})/2$. As one can see, the variation of the properties when the parameter m_2 varies in the admissible interval $m_2 \in [m_4, \sqrt{m_4}]$ is crucially important for the small values of the parameters m_2 and m_4 (i.e., when the composite properties are similar to those of the rank-1 laminate composite). However, this difference diminishes as parameters m_2 and m_4 increase, as can be seen in Fig. 7(b) where $m_4 \in [0.5, 1]$. Note that on the scale of Fig. 7(b), all of the curves in the interval $m_4 \in [0, 0.5]$ cannot be distinguished from the axis $d_{13} = d_{33} = 0$.

The coefficients d_{13} and d_{33} rapidly increase in the vicinity of the point $m_2 = m_4 = 1$. The general form of the dependence is similar for all of the three considered cases.

Therefore, for composites that are similar in properties to those of simple laminates (for example, composites with disk-like inclusions oriented perpendicular to the axes $\boldsymbol{k}$), the shape-dependence is crucial. For larger values of the structural parameter (when the composite properties approach those of fiber-reinforced composites), one can assign the intermediate value $m_2 = (m_4 + \sqrt{m_4})/2$ to the parameter m_2 and study the dependence of the properties on the remaining parameter m_4, since the variation of the properties with the parameter $m_2 \in [m_4, \sqrt{m_4}]$ is small.

Figure 8 shows the dependence of the effective parameters d_{13} and d_{33} on the structural parameter $m_4 \in [0, 1]$ (with m_2 being fixed at $m_2 = (m_4 + \sqrt{m_4})/2$) for several values of the volume fraction $f_2 = 0.1$, $f_2 = 0.4$, $f_2 = 0.8$, and $f_2 = 0.95$. It is seen that the effective piezoelectric coupling coefficients dramatically increase for all values of the volume fractions as the structure approaches that of fiber-reinforced composites ($m_2 = m_4 = 1$).

Figure 9 shows the dependence of the parameters d_{13} and d_{33} on the volume fraction f_2 for several values of the microstructural parameters $m_2 = m_4 = 0$ (laminate composites), $m_2 = m_4 = 1$ (fiber-reinforced composites), $m_2 = 2/3$, $m_4 = 8/15$ (isotropic tensor $\hat{\boldsymbol{Q}}$), and $m_2 = 0.979$, $m_4 = 0.963$ (epoxy composite reinforced by short fibers). Note that the fiber-reinforced composites possess the highest performance characteristics. If such a composite cannot be made, one should aim to increase the length of the fibers in the composite in order to improve the piezoelectric characteristics.

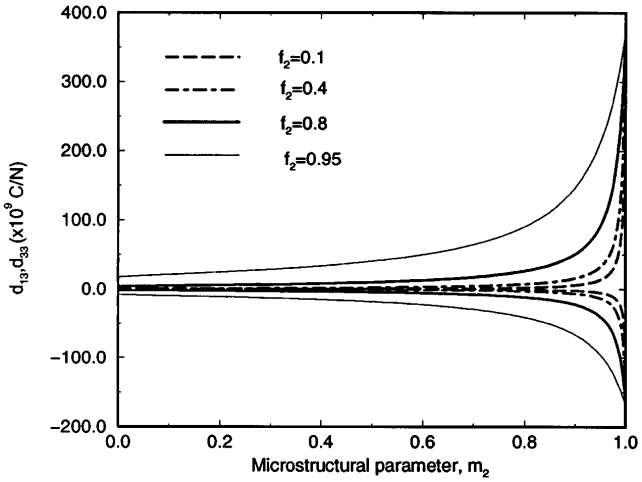

FIG. 8. The effective piezoelectric coefficients d_{13} and d_{33} of a PZT-5/epoxy composite as a function of the microstructural parameter m_4. The parameter m_2 is taken to be $m_2 = (m_4 + \sqrt{m_4})/2$.

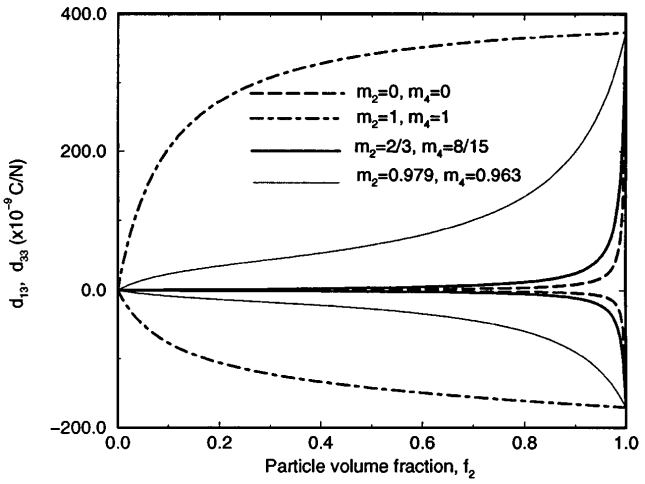

FIG. 9. The effective piezoelectric coefficients d_{13} (a) and d_{33} (b) of a PZT-5/epoxy fiber-reinforced ($m_2 = m_4 = 1$), short-fiber-reinforced ($m_2 = 0.979$, $m_4 = 0.963$), spherical-particles-reinforced ($m_2 = 2/3$, $m_4 = 8/15$), and laminate ($m_2 = m_4 = 0$) composites.

Let us now study the dependence of the parameters d_{13} and d_{33} on the stiffness of the matrix phase. We assume that the volume fraction of piezoelectric is equal to $f_2 = 0.1$, and the stiffness tensor of the matrix $\boldsymbol{C}_m$ is proportional to that of the epoxy, $\boldsymbol{C}_{ep}$, i.e., $\boldsymbol{C}_m = x\boldsymbol{C}_{ep}$. Thus, for $x = 1$, the properties of the matrix coincide with those given in Table I and the stiffness of the matrix increases with x. Figure 10 shows d_{13} and d_{33} as a function of $x \in [0, 5]$ for fiber-reinforced PZT-5/epoxy composite ($m_2 = m_4 = 1$). One can see that the performance slowly decreases with increase of x. The same is true for the other values of the microstructural parameters m_2 and m_4.

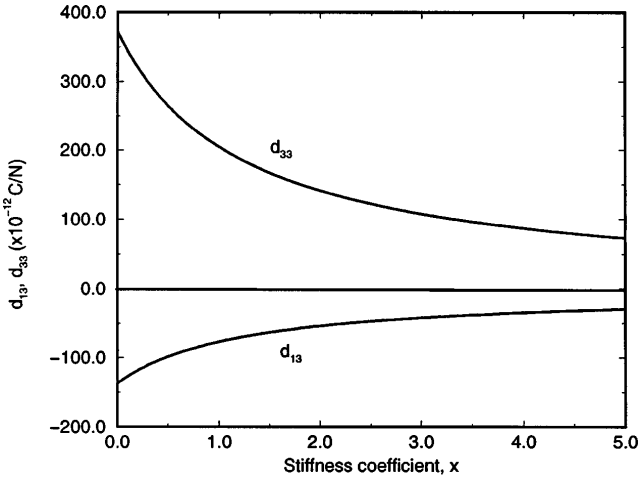

FIG. 10. The effective piezoelectric coefficients d_{13} and d_{33} of a fiber-reinforced composite ($m_2 = m_4 = 1$) PZT-5/epoxy composite as a function of the stiffness of the matrix, $\boldsymbol{C}_m = x\boldsymbol{C}_{ep}$. The inclusions volume fraction is equal to $f_2 = 0.1$.

V. CONCLUSIONS

We have derived exact analytical expressions for the effective moduli of the transversely isotropic matrix laminate composites consisting of transversely isotropic piezoelectric inclusions in an isotropic dielectric matrix phase. These formulas can be used to approximate the effective properties of any transversely isotropic dispersion.

It is shown that our expressions provide reasonable agreement with available experimental results. In the special case of spherical inclusions in a polymer matrix, our formulas agree with the Mori–Tanaka approximation for the effective moduli. Our formulas also coincide with the Mori–Tanaka approximation for the effective moduli of corresponding fiber-reinforced composites. We have proved that the Mori–Tanaka approximation for the effective piezoelectric moduli of dispersions of aligned spheroidal inclusions always can be realized by the MLC's. For this particular case we found simple relations between the aspect ratio of the spheroidal inclusions in the Mori–Tanaka scheme and the parameters m_2 and m_4 in or approximation. However, our formulas may differ from any of the known approximations when describing composites with more complicated microgeometries.

The advantage of our approximation is that it is (i) realizable, i.e., corresponds to specific microstructures; (ii) analytical and easy to compute even in non-degenerate cases; (iii) valid for the entire range of phase volume fractions; and (iv) characterized by two free parameters that allows one to "tune" the approximation and describe a variety of microstructures.

Our approximations allow one to adjust two microstructural parameters to provide good agreement with experimental or theoretical results for a wide range of volume fractions and arbitrary phase properties. These parameters depend only on the shape and size distribution of the inclusions and are independent of the phase properties and volume fractions. Finally, we have confirmed that among the considered class of composites the best performance characteristics are provided by the fiber-reinforced piezoelectric composite. The piezoelectric properties rapidly decay as the structure deviates from fiber-reinforced composites.

ACKNOWLEDGMENTS

The authors thank Robert Lipton for helpful discussions. This work was supported by the ARO/MURI Grant DAAH04-95-1-0102.

REFERENCES

1. K. A. Klicker, J. V. Biggers, and R. E. Newnham, J. Am. Ceram. Soc. **64**, 5 (1981).

2. R. E. Newnham and G. R. Ruschau, J. Am. Ceram. Soc. **74**, 463 (1991).
3. R. Y. Ting, A. A. Shalov, and W. A. Smith, Proc. 1990 IEEE Ultrason. Symp., 707 (1990).
4. M. J. Haun and R. E. Newnham, Ferroelec. **68**, 123 (1986).
5. H. L. W. Chan and J. Unsworth, IEEE Tran. Ultrason. Ferro. Freq. Control **36**, 434 (1989).
6. W. A. Smith, Proc. 1991 IEEE Ultrason. Symp., 661 (1991).
7. W. A. Smith, IEEE Tran. Ultrason. Ferro. Freq. Control **40**, 41 (1993).
8. M. L. Dunn and M. Taya, Int. J. Solids Struct. **30**, 161 (1993).
9. W. S. Kuo and J. H. Huang, Int. J. Solids Struct. **34**, 2445 (1997).
10. M. Avellaneda and P. J. Swart, working paper, Courant Institute of Mathematical Sciences (1993).
11. M. Avellaneda and T. Olson, *Recent Advances in Adaptive and Sensory Materials and Their Applications* (Technomic Press, Lancaster, PA, 1992).
12. Y. Benveniste, Mech. Mater. **18**, 183 (1994).
13. O. Sigmund, S. Torquato, and I. A. Aksay, J. Mater. Res. **13**, 1038 (1998).
14. L. V. Gibiansky and S. Torquato, J. Mech. Phys. Solids **45**, 689 (1997).
15. Z. Hashin, J. Mech. Phys. Solids **13**, 119 (1965).
16. G. Francfort and F. Murat, Arch. Rational Mech. Anal. **94**, 307 (1986).
17. Z. Hashin and S. Shtrikman, J. Appl. Phys. **35**, 3125 (1962).
18. Z. Hashin and S. Shtrikman, J. Mech. Phys. Solids **11**, 127 (1963).
19. J. R. Willis, J. Mech. Phys. Solids **25**, 185 (1977).
20. M. Avellaneda, SIAM J. Appl. Math. **47**, 1216 (1987).
21. K. A. Lurie and A. V. Cherkaev, Proc. Roy. Soc. Edinburgh A **104**, 21 (1986).
22. L. Tartar, in *Ennio de Giorgi Colloquium*, edited by P. Kree, Pitman Research Notes in Math. **125**, 168 (1985).
23. R. V. Kohn and G. W. Milton, J. Mech. Phys. Solids **36**, 597 (1988).
24. R. Lipton, J. Mech. Phys. Solids **39**, 663 (1991).
25. G. W. Milton, *Homogenization and Effective Moduli of Materials and Media*, edited by J. L. Ericksen, D. Kinderlehrer, R. V. Kohn, and J. L. Lions (Springer-Verlag, New York, 1986), p. 150.
26. T. Furukawa, K. Fujino, and E. Fukada, Jpn. J. Appl. Phys. **15**, 2119 (1976).
27. G. J. Weng, Int. J. Eng. Sci. **28**, 1111 (1990).
28. T. Mura, *Micromechanics of Defects in Solids*, 2nd ed. (Martinus Nijhoff, Dordrecht, The Netherlands, 1987).
29. Y. P. Qiu and G. J. Weng, Int. J. Eng. Sci. **28**, 1121 (1990).